X-ray stress measurement of carbide in tool steel

X-Ray Stress Measurement of Carbide in Tool Steel

Masahide Gotoh[1], Hajime Hirose[2] and Toshihiko Sasaki[3]

[1] Graduate school of Natural Science and Technology, Kanazawa University
Kakuma-machi, Kanazawa, Ishikawa 920-1192, Japan
[2]Research center, Kinjo University
1200 Kasama-machi, Matto, Ishikawa 924-8511, Japan
[3]Department of Materials Science and Engineering, Kanazawa University
Kakuma-machi, Kanazawa, Ishikawa 920-1192, Japan
[1]masahide@cs.s.kanazawa-u.ac.jp, [2]hirose@kinjo.ac.jp, [3]sasakit@kenroku.kanazawa-u.ac.jp

Keywords: Carbide, Stress measurement, Thin films, Substrate, Annealing, Misfit of plastic strain.

Abstract. Thin films deposited by physical vapor deposition (PVD) were studied in terms of residual stress by the authors. The final purpose of our study is to evaluate the stress state at the interface between a substrate and a thin film. In this study, JIS-SKH55 tool steel without thin-film deposition was used as the specimen. SKH55 is a dual-phase steel consisting of martensite α'Fe and alloyed carbide M_6C_2. The specimens were heated to 573K, 798K, 843K and 893K. Recently, the relationship between the misfit of plastic strain and stress obtained by X-ray stress measurement has been proposed by the authors using the Eshelby/Mori-Tanaka model (EMT model). The residual stress and the misfit of plastic strain were determined by X-ray stress measurement using the EMT model. Results showed that as annealing temperature increased, the compressive residual stress remained nearly constant up to about 800K, and decreased above 800K in both phases. The misfit of plastic strain also remained nearly constant up to about 800K, and reached zero above 800K.

Introduction

Tool steels are harder than carbon steels. Carbon in tool steels contributes to the hardness of the material. Martensite is a solid solution of carbon in ferrite. The lattice of martensite is distorted because carbon squeezes itself into the lattice of ferrite. Therefore, a dislocation slip in the martensite structure does not easily occur. It is difficult to deform the material plastically because of the increasing degree of dislocation. In addition, the presence of alloyed carbide in tool steels is related to the hardness of materials. The alloyed carbide is very hard and is as hard as martensite. Thus, the resulting material is very hard. However, the change in the volume fraction of the inclusion and the matrix, and the type of inclusion material could influence mechanical properties such as hardness [1]. On the other hand, it is considered that almost all tests on mechanical properties, such as tensile strength test and fatigue test, are related to the stress field in materials. X-ray stress measurement is a non destructive inspection method of stress field and it can measure every phase, inclusion and matrix. To date, thin films deposited by physical vapor deposition (PVD)

have been studied in terms of residual stress by the authors [2]. The substrate of the deposited specimen was JIS-SKH55 steel, and the materials of the thin films were TiN and TiCN. Specimens were annealed in a furnace at 573K, 798K, 843K and 893K. Results showed that the residual stress of thin films was very compressive at about –5GPa without annealing. As the annealing temperature increased, the compressive residual stress of thin films remained nearly constant up to 573K, and decreased at higher than 537K. However, the residual stress just under the thin films on the substrate was independent of annealing temperature.

In this study, JIS-SKH55 steel (equivalent to AISI M35) without thin-film deposition was used as the specimen. The inclusion was alloyed carbide M_6C_2, and the matrix was martensite α'Fe. The residual stress and the misfit of plastic strain were determined by X-ray stress measurement using the EMT model. The influence of annealing temperature on residual stress was investigated, and its influence of residual stress on the matrix of the inclusion was discussed.

Misfit of plastic strain

First, we described an outline of the misfit of plastic strain measurement by Sasaki et al. In X-ray stress measurement, the stress in each phase of a composite material can be measured separately. The stress in each phase, called 'phase stress', can be determined using the X-ray diffraction profile from each phase. Macro stress can also be measured using

$$(\sigma_{11}^0 - \sigma_{33}^0) = (1-f)(\sigma_{11}^M - \sigma_{33}^M) + f(\sigma_{11}^I - \sigma_{33}^I), \tag{1}$$

where σ^0 is the macro stress, σ^M is the phase stress of the matrix, σ^I is the phase stress of the inclusion and f is the volume fraction of the inclusion. In this study, the α'Fe phase is determined as the matrix, and the M_6C_2 phase is determined as the inclusion. Otherwise, phase stress is described by micromechanics, which considered in Eshelby's approach and the Mori-Tanaka theory.

$$\sigma_{11}^M - \sigma_{33}^M = 3U(\sigma_{11}^0 - \sigma_{33}^0) - 3B_1 f(\Delta\varepsilon_{11}^{\mathrm{P}} - \Delta\varepsilon_{33}^{\mathrm{P}}), \tag{2}$$

$$\sigma_{11}^I - \sigma_{33}^I = 3U^*(\sigma_{11}^0 - \sigma_{33}^0) - 3B_1(1-f)(\Delta\varepsilon_{11}^{\mathrm{P}} - \Delta\varepsilon_{33}^{\mathrm{P}}). \tag{3}$$

Here, $\Delta\varepsilon^{\mathrm{P}} = \varepsilon_{11}^{\mathrm{P}} - \varepsilon_{33}^{\mathrm{P}}$ is determined as the misfit of plastic strain by

$$\Delta\varepsilon^{\mathrm{P}} \equiv \varepsilon_I^{\mathrm{P}} - \varepsilon_M^{\mathrm{P}}. \tag{4}$$

From Eq. 2 and 3, $\Delta\varepsilon^{\mathrm{P}}$ has following form:

$$\Delta\varepsilon_{11}^{\mathrm{P}} - \Delta\varepsilon_{33}^{\mathrm{P}} = \frac{U}{Q}(\sigma_{11}^I - \sigma_{33}^I) - \frac{U^*}{Q}(\sigma_{11}^M - \sigma_{33}^M), \tag{5}$$

where U, U^* and Q are determined by

$$U=\frac{\mu-\beta(\mu-\mu^*)}{3B},\ U^*=\frac{\mu^*}{3B},\ Q=B_1\{3U(1-f)+3U^*f\},\ B_1=\frac{2(\beta-1)\mu\mu^*}{3B},$$

$$\mu=\frac{E}{2(1+\nu)},\ \mu^*=\frac{E^*}{2(1+\nu^*)},\ B=\mu-\{\beta-f(\beta-1)\}(\mu-\mu^*),\ \beta=\frac{2(4-5\nu)}{15(1-\nu)}, \quad (6)$$

where E and E^* are Young's moduli, and ν and ν^* are Poisson's ratios of the matrix and the inclusion, respectively. The misfit of plastic strain $\Delta\varepsilon^P$ can be calculated using Eq. 5 with the phase stress measurement of each phase. Young's modulus and Poisson's ratio were obtained from the literature [3].

Experimental

Specimen. JIS-SKH55 steel (AISI M35) was used as the specimen. Figure 1 shows a scanning electron microscopy (SEM) image of the specimen. Spherical alloyed carbides of approximately 1μm diameter were distributed in the martensite. The specimen is 12x12x5 mm^3. The surface of the specimen was polished to the same roughness as the specimen for thin-film experiments, because a comparison between the deposition and non deposition cases is intended. The JIS-SKH55 used was composed of C=0.9mass%, Cr=4.2mass%, Mo=5.0mass%, W=6.2mass%, V=2.0mass% and Co=5.0mass%. Regarding heat treatments, one of the specimens was left at room temperature, while the others were annealed in a furnace. Annealing time was 3.0 hours. Heat treatment conditions for each sample are listed in Table 1.

X-ray stress measurement. Stress measurement by X-ray diffraction provides stress/strain information concerning the surface of materials. The equipment used for the stress measurement was MSF-2M (RIGAKU Corp., Japan). An irradiated beam of dimension was 4x6 mm^2. Table 2 lists the measurement conditions for X-ray stress measurement.

Table 1 Heat treatment conditions

Temperature	300K	573K	798K	843K	893K
Atmosphere	----------	Air	Vacuum (1.33Pa)	Vacuum (1.33Pa)	Vacuum (1.33Pa)

Table 2 X-ray stress measurement conditions

	α'Fe	M_6C_2
Characteristic radiation	Cr-Kα	
Tube voltage [kV]	30	
Tube current [mA]	10	
Kβ filter	V	
Diffraction plane	211	822
Diffraction angle 2θ [deg]	156.41	122.67

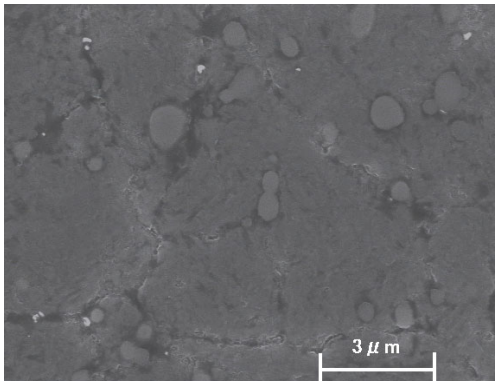

Fig. 1 SEM image of specimen

Hardness test. Rockwell hardness test was carried out, because it was confirmed that the relationship between hardness and annealing temperature. Rockwell C scale was applied, and the holding time was 30 seconds.

Results and discussion

Observation of X-ray profiles. Figure 2 shows the X-ray profiles obtained from the specimen. Peaks of α'Fe were clear. For the alloyed carbide phase, the peak intensities were very small. However, if only it takes long time, the stress of carbide phase can be measured sufficiently.

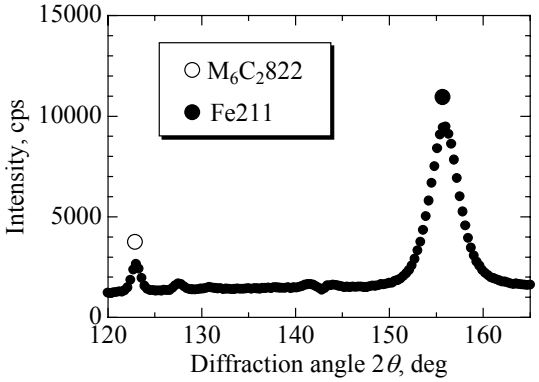

Fig. 2 X-ray profile of specimen

Experiment using bending machine. The relationship between applied stress using bending machine and measured stress by X-ray was investigated. Tensile applied strains ε_{APP} were 0, 250 and 500 x10^{-6}. The $\sin^2\psi$ diagrams are shown in Fig. 3. A straight line could be drawn approximately on the plots. Therefore, the stress could be determined by the $\sin^2\psi$ method for the carbide phase. However, the stress of the martensite phase could be measured easily. Because the specimen surface was polished, there was compressive residual strain in both phases despite the applied strain ε_{APP}.

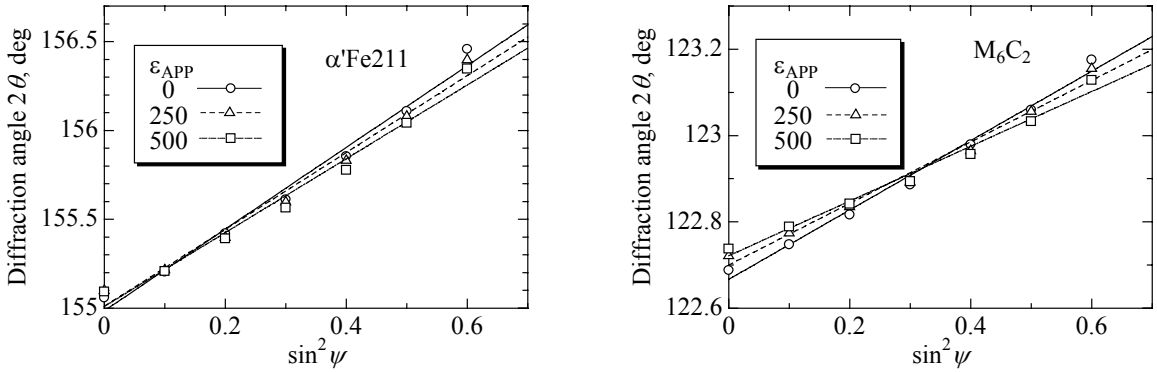

(a) Martensite phase (b) Carbide Phase

Fig. 3 $\sin^2\psi$ diagrams obtained by experiment of bending test

Figure 4 shows the relationship between the applied strain ε_{APP} and the slope M in 2θ-$\sin^2\psi$ diagrams. The X-ray elastic constant of the composite material (CXEC) was calculated from Fig. 4. However, the X-ray elastic constant of the phase material (PXEC) is required in stress calculation [4]. The equation between PXEC and CXEC is determined by

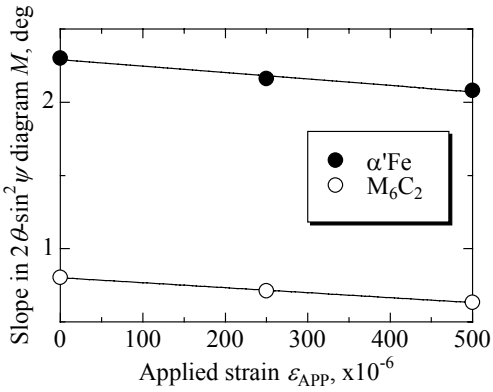

Fig. 4 Change in M with applied strain

$$\frac{(S_2^I)_{composite}}{(S_2^I)_{phase}} f + \frac{(S_2^M)_{composite}}{(S_2^M)_{phase}} (1-f) = 1, \tag{7}$$

$$S_2 = \left(\frac{2(1+\nu)}{E} \right)_{X-ray}, \tag{8}$$

where S_2 is the X-ray elastic constant shown in Eq. 8. E and ν in Eq. 8 depend on the diffraction plane and are different from those in Eq. 6. The superscripts of S_2^M and S_2^I indicate 'matrix' and 'inclusion', respectively. $(S_2^M)_{composite}$ and $(S_2^I)_{composite}$ were measured from Fig. 4. In addition, $(S_2^M)_{phase}$ was calculated using the Kröner model with the elastic compliance of the α'Fe single crystal. However, there is no bulk material of cemented carbide. Therefore, $(S_2^I)_{phase}$ could be obtained using Eq. 7. The volume fraction of inclusion f was measured by the point count method, and f was determined to be 0.124. The stress constant of the $M_6C_2$822 plane was calculated as $K_{carbide}$= -2242.71MPa/deg.

Change in residual stress due to annealing temperature. Figure 5 shows the relationship between residual stress and annealing temperature. Specimens without annealing were given compressive residual stress by polishing. As annealing temperature increased, the compressive residual stress remained nearly constant up to about 800K, and decreased at temperatures higher than 800K in both phases. Also, variation tendency of the other X-ray parameter, the full-width at half maximum (FWHM) of the X-ray profile, was similar to the variation tendency of the residual stress. The FWHM remained nearly constant up to 800K, and decreased at higher than 800K. The third kind stress is the deviation from the average stress within regions smaller than a grain, and the strength of the stress is similar to the atomic force. They are caused by lattice defects, dislocations and other factors. The presence of the third kind stress is evaluated qualitatively by changes in FWHM. A decrease in FWHM results from a decrease in the third kind residual stress due to annealing. The relaxation of compressive residual stress may be related to the relaxation of the third kind residual stress in grains.

Rockwell hardness test. Figure 6 shows the relationship between the Rockwell hardness (HRC) and annealing temperature of specimens.

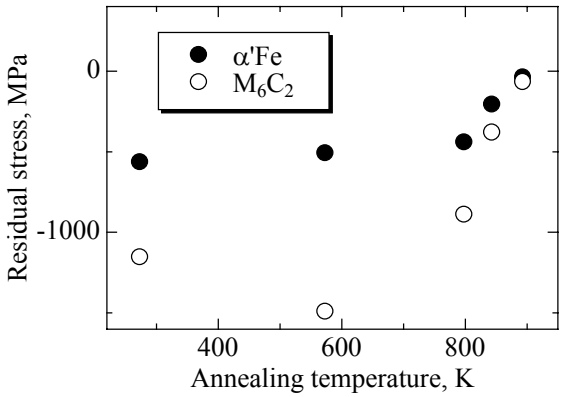

Fig. 5 Change in residual stress with increasing annealing temperature

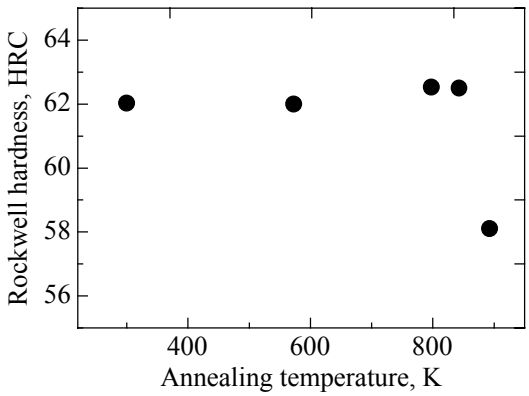

Fig. 6 Change in hardness with increasing annealing temperature

As annealing temperature increased, the Rockwell hardness remained nearly constant up to 843K, and decreased at temperatures higher than 843K. The variation in the hardness did not correspond to the variation in the stress obtained by experiments using X-ray. It is generally known that JIS-SKH55 becomes soft at about 873K, and this experimental result agrees with general report. The reasons it becomes soft with annealing are the expansion of grains due to condensation and the appearance of carbides in the grains. Therefore, it was confirmed that the temperature at which residual stress changes is lower than that at which hardness changes. This phenomenon should be very important when we study the fatigue strength of this material, because it has two causes for fatigue fracture.

Evaluation by misfit of plastic strain. Figure 7 shows the relationship between the misfit of plastic strain and annealing temperature. As annealing temperature increased, the misfit of plastic strain remained nearly constant up to 800K, and decreased at temperatures higher than 800K. The plastic strain was generated by polishing, and was reduced by annealing. In addition, it is confirmed by Eq. 4 that the plastic strain of the inclusion is larger than that of the matrix. Because the residual stress and the misfit of plastic strain are independent, fatigue problems in both phases should be considered in the case of a prolonged fatigue process.

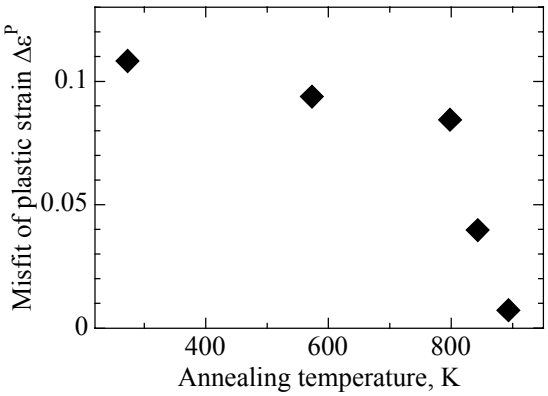

Fig. 7 Change in misfit of plastic strain with increasing annealing temperature

Summary

(1) In the case of using non-deposited thin films, as annealing temperature increased, the compressive residual stress remained nearly constant up to about 800K, and decreased at temperatures higher than 800K in both martensite and alloyed carbide phase. (2) As annealing temperature increased, the Rockwell hardness remained nearly constant up to 843K, and decreased at temperatures higher than 843K. (3) As annealing temperature increased, the misfit of plastic strain remained nearly constant up to 800K, and decreased at temperatures higher than 800K. The plastic strain of the inclusion was larger than that of the matrix.

Acknowledgement

Thank Mr. Matsumoto (Undergraduate school, Kanazawa university) for his support of this work.

References

[1] M.Nishida, T.Hanabusa and H.Fujiwara: J. Soc. Mat. Sci. Japan Vol.38 (1989), pp.576-581

[2] M.Gotoh, T.Sasaki and Y.Hirose: J. Soc. Mat. Sci. Japan Vol.52 (2002), pp.744-749

[3] M.Umemoto and K.Tsuchiya: Tetsu-to-Hagane Vol.88 (2002), pp.117-128

[4] K.Tanaka, N.Mine and K.Suzuki: J. Soc. Mat. Sci. Japan Vol.39 (1990), pp.1235-1241